Journal of Microwaves, Optoelectronics and Electromagnetic Applications, Vol. 21, No. 4, December 2022
DOI: http://dx.doi.org/10.1590/2179-10742022v21i4264212

Single Port Multimode Reconfigurable UWB-NB Antenna for Cognitive Radio Applications

Bhushan V. Kadam[1], Lucy J. Gudino[2], Ramesha C. K.[1], Joseph X. Rodrigues[3]
[1]*Department of Electrical and Electronics Engineering, BITS Pilani, K. K. Birla Goa Campus, Goa, India*
p20130010@goa.bits-pilani.ac.in, rameshack@goa.bits-pilani.ac.in
[2]*Department of Computer Science and Information Systems, BITS Pilani, Pilani, India*
lucy.gudino@pilani.bits-pilani.ac.in
[3]*Department of Electrical and Electronics Engineering, Christ University, Bengaluru, India*
joseph.rodrigues@christuniversity.in

***Abstract*— In this paper, a compact, single port, multimode reconfigurable UWB-NB antenna with a novel feeding network is presented. The proposed antenna consists of a pentagonal-shaped monopole radiator, a beveled-shaped partial defected ground plane with a rectangular slot, and a reconfigurable bypass feeding network. The antenna realizes a wideband frequency range from 2.4 to 18 GHz and four narrow band frequency ranges, 5.3 to 6.8 GHz, 6.0 to 7.6 GHz, 7.2 to 8.8 GHz and 8.4 to 11.4 GHz. The antenna provides an omnidirectional radiation pattern with gain from 2.2 to 6.2 dBi maximum at 12 GHz and voltage standing wave ratio (VSWR) ranges from 1 to 2. The fabricated antenna has an overall dimension of $18\times21\times1.6$ mm^3. Sensing and tuning ranges of the fabricated antenna shows good agreement with the simulation results. The proposed antenna has an advantage of simple design, low profile, single port excitation and omnidirectional radiation pattern making it suitable for applications such as handheld mobile cognitive radio systems.**

***Index Terms*—** Monopole, Cognitive radio, Ultrawideband (UWB), Reconfigurable antenna, Feeding network.

I. INTRODUCTION

With rapid development in modern communication systems, the limited electromagnetic spectrum has become more and more congested. On the other hand, it is broadly perceived that the existing allocated spectrum is far from being efficiently utilized. The techniques on dynamic spectrum management, efficient allocation and utilization has drawn much attention due to the congested spectrum [1]. Cognitive Radio (CR) offers one of the most efficient solutions to realize dynamic spectrum sensing with improved spectral efficiency [2]. The CR system can dynamically sense spectrum within a wideband range and provide services by allocating frequency band from unoccupied spectrum without causing interference to other users [3]. Antennas are the front end of the CR system. Antenna design for CR applications has been a research hotspot for several years. Traditionally, two separate antennas namely, Ultrawideband (UWB) antenna for spectrum sensing and Narrowband (NB) frequency reconfigurable antenna for communication connected to two different ports is used. In general, UWB antennas are bigger than NB antennas, which will be a significant problem for handheld mobile devices. Hence, the focus is on

Brazilian Microwave and Optoelectronics Society-SBMO *received 21 May 2022; for review 5 June 2022; accepted 24 Oct 2022*
Brazilian Society of Electromagnetism-SBMag *ISSN 2179-1074*

developing a single port, compact antenna which can provide both the UWB and NB characteristics, and support multimode operation.

There are several antenna designs available in the literature that make use of PIN diodes and/or varactor diodes to achieve frequency reconfiguration. The hexa-band frequency reconfigurable antenna proposed in [4] achieves two single band modes, and two dual band modes by changing the states of PIN diodes. The cavity slot patch antenna consisting of four PIN diodes, produces multiband frequency of operation with 12 bands [5]. In [6], PIN diodes are used to switch between four different frequency bands by exciting the antenna through a Reconfigurable Bandpass Filter (BPF). In [2], the frequency tuning range from 3.85 to 5.94 GHz is achieved by using a T-shaped and H-shaped resonator loaded with a varactor diode. In [7], the antenna consists of a rectangular microstrip patch with a pair of varactor diodes embedded onto Defected Ground Structure (DGS). The varactor diode changes the current distribution around the defect, producing a tuning range from 5 to 6.7 GHz. In [8], four symmetric resonators are connected to the central rectangular shaped patch via varactor diodes. Here, the operating frequency varies continuously by altering the bias voltages on varactor diodes. The use of varactor diodes provide non-linear operation with a low dynamic range [2], [7], [8]. On the other hand, the PIN diode is a common choice to realize UWB frequency reconfiguration due to their advantages such as reliability and extremely low cost. Performance comparison of the NB frequency reconfigurable antennas is summarized in Table I.

TABLE I. PERFORMANCE COMPARISON OF FREQUENCY RECONFIGURABLE NB ANTENNAS

Ref.	**Size** (mm^3)	**Frequency reconfiguration technique**	**Active Components (#)**	**NB range (GHz)**
[2]	40×40×0.8	T and H shaped BPF integrated onto the feedline	Varactor diode (2)	3.85-5.58
[4]	33×16×1.6	By changing the length of the resonator	PIN diode (3)	2.1, 4.5 and 2.4, 5.2
[5]	40×47×1.6	Substrate integrated waveguide cavity with C and E shaped slots	PIN diode (5)	2.624-5.392
[6]	30×60×1.6	Reconfigurable BPF integrated onto the Transmission Line	PIN diode (4)	1.8, 2.4, 3.5 and 5.2
[7]	30×30×1.6	Rectangular slot in ground plain	Varactor diode (2)	4.65-6.18
[8]	34×38×1.6	Four parasitic patches connected to the driven element	Varactor diode (4)	3.29-4 and 5.35-7

To minimize the size and cost due to multiple antennas in the CR system, several techniques have been proposed. In those techniques two or more antennas are integrated into a single substrate using different ports. The concept of integration of multiport antennas is described in [9], where wideband to NB transition is achieved. In [10], NB antenna elements are integrated with an UWB sensing antenna by using PIN diodes and varactor diodes to cover an operating range from 0.72 to 3.44 GHz. Gandhi et al., presented four port [11] and five port [12] integrated UWB and NB antenna for CR systems. Both the designed antennas cover the entire UWB range of 3.1 to 10.6 GHz for sensing as well as communication purposes.

Even though multiport antenna designs have the advantage of achieving a wide operating frequency range, it requires a complex switching network to operate between different NB antenna elements. To overcome the limitation of multiport and complexity involved in switching, a dual port UWB Dielectric Resonator Antenna (DRA) is integrated with frequency reconfigurable NB antenna [13]. The designed

received 21 May 2022; for review 5 June 2022; accepted 24 Oct 2022

ISSN 2179-1074

antenna provides a wide tunable bandwidth from 3.25 to 8.4 GHz achieved by switching the PIN diodes.

The dual and multiport antenna system enables simultaneous sensing and communication over the channel. To reduce the size of the overall antenna system, individual radiators are closely placed which produces high mutual coupling due to which isolation level is reduced between the radiators. This inturn increases the interference between the antennas. Hence, there is a compromise between the overall size and the isolation level. In recent years, research activities have been conducted to combine UWB and frequency reconfigurable NB antennas excited by using a single port feed [3], [14]–[16].

The single port antenna design is more challenging. In [15], a frequency selective antenna composed of a monopole patch and a reconfigurable filter in the ground plane. The designed antenna is tuned to wideband mode or NB mode by using four horizontal slots integrated with 16 PIN diodes. The antenna design presented in [14] achieves UWB to NB and UWB to dual-band resonance by using ideal switches to activate different resonating stubs. A wideband to NB frequency reconfiguration is also possible by using a combination of PIN and varactor diodes. In [16], the frequency reconfigurable DRA with 3.82 to 8.94 GHz sensing range and 5.14-5.98 GHz communication range is presented. Three PIN diodes are employed to switch between wide and narrow band operational modes and the varactor diode is used to tune the operational frequencies continuously. In [3], a reconfigurable antenna uses a tunable bandpass filter with PIN diode for wideband to narrow band switching and two varactor diodes are used to continually alter the antenna communication frequency from 3.9 to 4.82 GHz.

The performance of the antenna designs in terms of size, antenna technique, switching technique, number of ports and operating range is presented in Table II.

It is evident from the table that the communication range is limited as compared to the sensing range [3], [9], [14]–[16]. Designing a single port, compact, reconfigurable, single UWB-NB antenna with a large communication range is a challenging task. Hence, to address this issue, in this paper, we propose a single port, compact, multimode UWB-NB antenna to be used in handheld portable cognitive radio applications.

Rest of the paper is organized as follows. Section II presents the proposed UWB-NB antenna evolution, performance study of each evolution stage and antenna equivalent circuit. Section III presents design and analysis of the proposed reconfigurable UWB-NB antenna. Detailed simulated and measured results are also discussed in this section. Section 4 presents a brief conclusion.

Brazilian Microwave and Optoelectronics Society-SBMO *received 21 May 2022; for review 5 June 2022; accepted 24 Oct 2022*
Brazilian Society of Electromagnetism-SBMag *ISSN 2179-1074*

TABLE II. PERFORMANCE COMPARISON OF MULTIMODE UWB ANTENNAS

Ref.	Size (mm^3)	Frequency reconfiguration technique	No. of ports	Active components	UWB range (GHz)	NB range (GHz)
[3]	30×65×0.8	Three-line coupled resonator integrated onto feedline	1	PIN (1) and varactor (2)	3.5-5.5	3.9-4.82
[9]	36×54×0.8	Shorted microstrip patch integrated with a CPW fed monopole	2	NA	3.1-10.6	4.9-5.35, 8 and 10
[10]	65×120×1.6	Meander-line planar antenna integrated onto UWB sensing antenna	3	PIN (2) and varactor (2) diode	0.72-3.44	0.57-2.55
[11]	28×31×1.6	1 UWB and 3 NB monopole resonators integrated onto single substrate	4	NA	2.9-13.1	3.06-4.49, 4.29-6, 5.97-8.35, and 8.26-11.16
[12]	40×36×1.6	1 UWB and 4 NB monopole resonators integrated onto single substrate	5	NA	3.1-10.6	3.06-4.23, 4-6.36, 6.33-8.33, 8.7-9.92 and 9.82-10.74
[13]	65×40×6.5	Rectangular DRA integrated with a reconfigurable NB antenna	1	PIN (2)	3.0-11.0	3.4-3.65, 5.5-6.5 and 8-8.4
[14]	40×60×1.6	C and T-shaped stub resonators integrated onto TL	1	Ideal switches (5)	3.2-12.0	3.31 and 5.1
[15]	68×68×1.6	Inverted U-shaped radiator with 4 slots in ground	1	PIN (12)	2.63-3.7	2.6-3.4
[16]	24×32×1.0	Rectangular DRA excited by microstrip feedline with a reconfigurable filter	1	PIN (3) and varactor(1) diode	3.82-8.94	5.22-6.07
This work	18×21×1.6	Pentagonal monopole excited by reconfigurable bypass feed	1	PIN (12)	2.4-18	5.3-6.8, 6-7.6, 7.2-8.8 and 8.4-11.4

II. UWB-NB ANTENNA DESIGN

The proposed antenna structure is divided into two parts, UWB antenna for spectrum sensing and reconfigurable NB antenna for communication purposes. In this section, the design of the proposed UWB-NB antenna is presented. The proposed antenna design is evolved through the four different configurations. The configuration-I uses a rectangular monopole patch with a partial rectangular ground plane. Configuration-II uses a pentagonal shaped radiating patch with a partial rectangular ground plane. Configuration-III uses pentagonal-shaped radiating patch with beveled-shaped ground plane, whereas Configuration-IV uses pentagonal-shaped radiating patch with rectangular slot added on the beveled-shaped ground plane. The simulation of the four antenna configurations has been performed using Ansys High Frequency Structure Simulator (HFSS) and performance is evaluated. Also, a brief analysis is presented for selecting appropriate antenna substrate material. For all the four configurations, simulation is performed using FR4 glass epoxy substrate with the following properties: dielectric constant ϵ_r = 4.4, thickness h = 1.6 mm, and loss tangent $\tan\delta$ = 0.02. A brief analysis is presented for selecting FR4 substrate for designing the proposed antenna. A detailed analysis of simulation results has been done for all the four configurations.

A. Selection of substrate material

FR4 substrates are generally used for designing the antennas at microwave frequencies due to their advantages such as low cost and easy availability. However, FR4 material shows the dielectric constant

Brazilian Microwave and Optoelectronics Society-SBMO *received 21 May 2022; for review 5 June 2022; accepted 24 Oct 2022*
Brazilian Society of Electromagnetism-SBMag *ISSN 2179-1074*

variation as a function of position, frequency, and temperature. To overcome this, for large batch manufacturing low loss FR4 substrates can be used. On the other hand substrates like RO3003^{TM} [2], RT duriod 5880 [3], [5], [7], and Taconic TLC [9] are having stable dielectric constant and very low loss tangent but are expensive. For quarter wavelength microstrip antenna for minimum resonance frequency (f_L), the length (L) can be determined by using guided wavelength (λ_g) and is given by,

$$\lambda_g = \frac{c}{4f_L\sqrt{\varepsilon_{eff}}} \tag{1}$$

where, c is the speed of light and ϵ_{eff} = (ϵ_r + 1) / 2 is the effective dielectric constant. By using (1), the analysis has been done for different substrate materials operating at minimum frequency of f_L = 3 GHz. Among all the substrate materials, the RT/duriod 5880, RO3003^{TM} and Taconic TLC has the lower $\tan\delta$ as compared to FR4 substrate with high stability in effective dielectric constant ε_{eff}. Therefore, these materials are highly suitable for satellite, space, and mission critical applications [17]. Through the detailed literature survey it is observed that except for references, [2], [3], [5], [7], [9] all the reported antenna uses commonly available low cost FR4 substrate. Therefore, in the proposed antenna design FR4 substrate material is used due to its advantages of low cost, easy availability, and compact antenna size.

The multimode reconfigurable UWB-NB antennas are highly suitable for CR applications. However, it is very challenging to design and develop low cost, efficient, and improved UWB-NB antenna system for CR applications. Microstrip antennas provide easy integration with other microwave integrated components and electronics circuits on the same substrate board. Therefore, the overall size of the Printed Circuit Board (PCB) is also an important design aspect. The standard UWB radio system such as Decawaves DW1000 UWB transceiver IC with FR4 substrate uses the dielectric chip antenna ACS5200HFAUWB. This chip antenna operates from 3.2 to 7.2 GHz with a peak gain of 4.16 dB at 6.2 GHz. The overall space required to mount the chip antenna is 13 mm$\times$23 mm with 28.5 mm vertical spacing on both sides of the antenna for proper radiation. As per the amendment to the revision of 802.16.2-2001 standard to expand its scope to support cognitive radio and network frequencies from 2 to 11 GHz [18]. However, the bandwidth of the chip antenna is less as compared to the proposed antenna and it is not reconfigurable.

B. Proposed UWB sensing antenna design

This subsection presents the four evolutions of the proposed UWB antenna used for CR sensing with their advantages, disadvantages, and frequency of operation. The optimal values for all the antenna design parameters are obtained from monopole antenna equations and parametric analysis performed using Ansys HFSS.

First step is to find out antenna patch shape, ground shape and overall dimensions of the antenna. For a cylindrical monopole antenna, the lower cut-off frequency corresponding to Voltage Standing Wave Ratio (VSWR) $\leq$ 2 can be approximately calculated by (2) [19],

$$f_L = \frac{7.2}{L + r + p} \tag{2}$$

where, L is the length of the cylindrical monopole antenna, r is the radius of the cylindrical monopole antenna, and p is the feed length in cm. As shown in Fig. 1, the Configuration-I antenna design starts

Brazilian Microwave and Optoelectronics Society-SBMO *received 21 May 2022; for review 5 June 2022; accepted 24 Oct 2022*
Brazilian Society of Electromagnetism-SBMag *ISSN 2179-1074*

with basic rectangular monopole design which consists of a rectangular monopole patch fed by 50 Ω feed line and a partial rectangular ground plane at the bottom of the substrate. The dimensions of the rectangular monopole antenna is calculated by equating its area to that of an equivalent cylindrical monopole antenna of the same length (L) and $r = W/2\pi$. As per the (1), length of the Configuration-I antenna patch is 15 mm at the lower UWB cut off frequency of 3.1 GHz. By putting this value in (2), the estimated value of W = 10 mm and length of the 50 Ω feed line is 6 mm. The width of the backside partial ground plane is optimized to 16 mm. Therefore, the overall dimensions of the antenna becomes $18\times21\times1.6$ mm^3.

Fig. 1 and Fig. 2 show the VSWR and reactance plot respectively for antenna configurations-I. It can be observed from both the plots that, between patch and the ground, the antenna has a strong mutual coupling resulting in poor impedance matching. Poor impedance matching is significantly below 12 GHz which is mainly due to abrupt variation in impedance at the interface of the rectangular monopole patch and the feed line. Strong mutual coupling leads to higher values of inductive and capacitive reactance at lower frequencies. Antenna Configuration-I provides dual bands and resonates at 3.2 to 6 GHZ and 11 to 13.5 GHz.

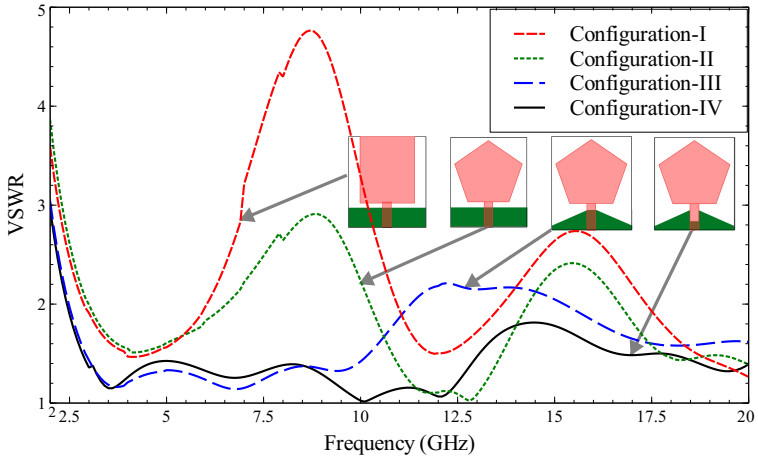

Fig. 1. VSWR in the different antenna configurations.

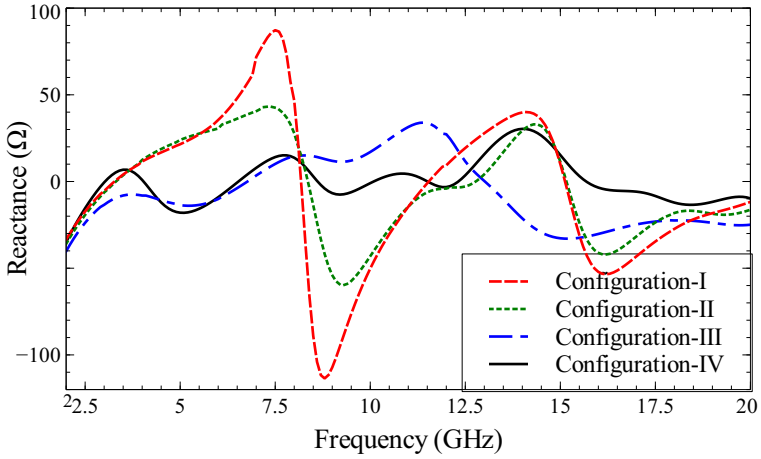

Fig. 2. Reactance plot in the different antenna configurations.

In order to improve the impedance matching, in antenna Configuration-II, the rectangular-shaped

ISSN 2179-1074

patch is replaced by the pentagonal-shaped radiating patch of length L_P with the same aperture area. It is observed from Fig. 1 and Fig. 2 that, at frequencies below 12 GHz, the reactance is reduced as compared to Configuration-I. The antenna resulted in dual band resonance from 3 to 6.5 GHz and from 10.5 to 14 GHz. This improved performance is mainly due to the partial rectangular ground plane coupled to the radiating patch.

To further improve the performance of the antenna, the rectangular-shaped ground plane is replaced by the bevel-shaped defected ground in antenna Configuration-III. It can be seen that the beveled-shaped defected ground plane not only improved the impedance matching at the lower frequencies but also improved frequency range from 2.7 to 10 GHz and 15 to 18 GHz. However, the reactance is still significant in antenna Configuration III. To further improve impedance matching, the rectangular slot of length G_{sL} has been added to the beveled defected ground plane in antenna Configuration-IV. Due to this, the surface area of conducting plates between ground and feed line is reduced, which results in a reduction of the capacitive reactance. The VSWR curve in Fig. 1 shows that the antenna in configuration-IV achieves a wide bandwidth from 2.4 to 18 GHz. Fig. 3 shows the geometrical design of the proposed UWB sensing antenna. The optimized dimensions of the proposed antenna (in mm) are summarized in Table III.

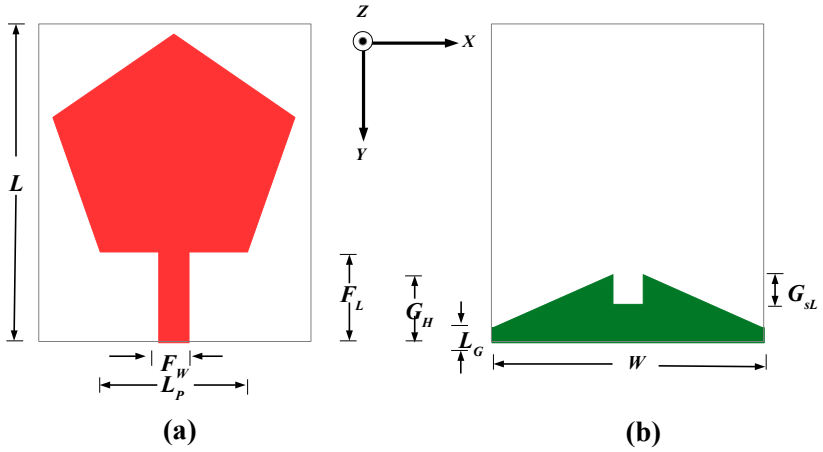

Fig. 3. Geometry of the proposed UWB antenna (a) Top view and (b) Bottom view.

TABLE III. PHYSICAL DIMENSIONS OF THE PROPOSED ANTENNA

Parameter	Description	Size (mm)	Parameter	Description	Size (mm)
L	Length of the antenna	21	W	Width of the antenna	18
L_P	Length of the pentagonal-shaped patch	8	F_L	Microstrip feed length	5.8
F_W	Microstrip feed width	2	G_H	Ground plane height	4.5
L_G	Ground length	1	G_{sL}	Ground slot length	1

C. Antenna design using variable bypass feed

Instead of developing a separate NB antenna for communication purposes, the existing UWB sensing antenna can be modified to generate NB frequency. To achieve this, a variable bypass feed line having a length BF_L is included in the UWB sensing antenna. The width of the bypass feed line is set to 0.5 mm. Fig. 4 shows the structure of the bypass feed line. Rectangular slot of length S_W is added to the

feed line which will help in blocking the signal coming from main feed so that signal to the antenna is fed only by the bypass feed line.

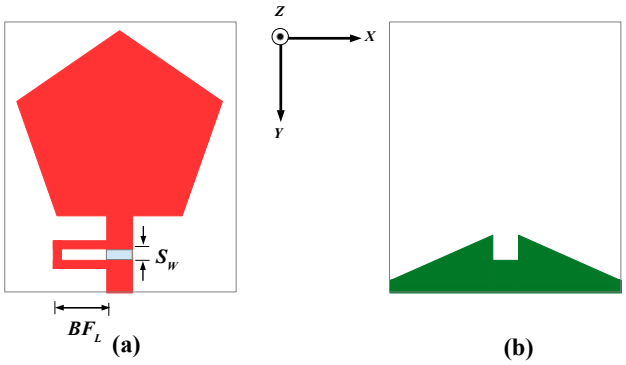

Fig. 4. Geometry of the variable bypass feed antenna (a) Top view and (b) Bottom view.

The tuning of the narrow frequency band is achieved by adjusting the length BF_L of the bypass feed line. Fig. 5 shows the plot of HFSS simulated reflection coefficient (S_{11}) for different lengths of bypass feed line. It is evident from the plot that the length of the bypass feed BF_L has a direct impact on operating frequencies of the antenna. The modified antenna structure achieves overlapping lower frequency bands and non-overlapping higher frequency bands for different values of BF_L. Hence, four distinct bands covering from 5.3 to 11.4 GHz are achieved by using the variable bypass feed.

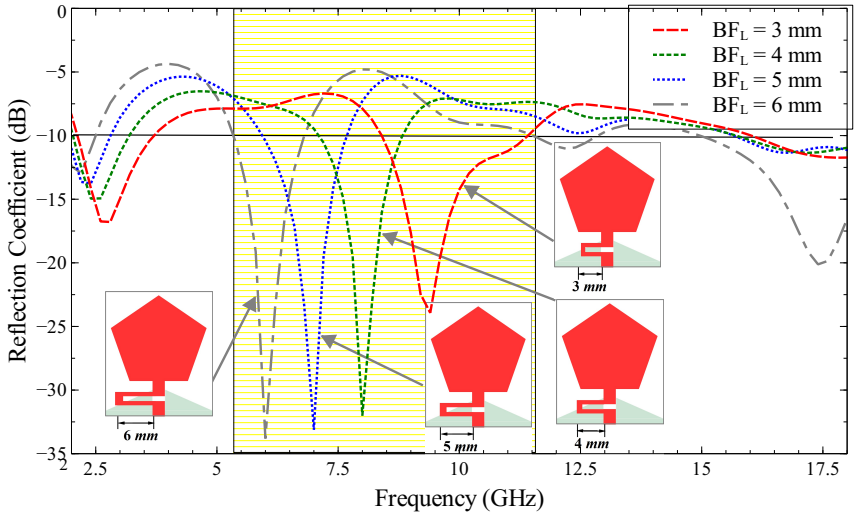

Fig. 5. Simulated reflection coefficient for different values of bypass feed length.

D. Equivalent Circuit Model

To further evaluate the tuning capability of the proposed antenna for different values of BF_L, the equivalent circuit model is implemented using Keysight's PathWave Advanced Design System (ADS) is presented. The antenna reflection coefficient response and impedance plot is used to obtain the equivalent circuit model. The model is represented using a lumped circuit with two parallel RLC (PRLC) resonators as shown in Fig. 6. The PRLC1 resonator is meant to operate at lower band, while the PRLC2 at higher band. The model is used to depict any drop in the reflection coefficient below

received 21 May 2022; for review 5 June 2022; accepted 24 Oct 2022

ISSN 2179-1074

−10 dB. This model also estimates the sharpness of the resonating bands by computing the quality factor (Q_0) of the resonating bands.

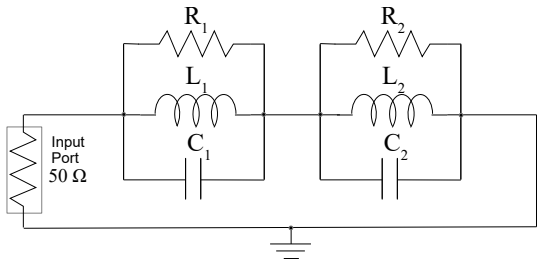

Fig. 6. Antenna equivalent circuit.

The following equations are used to calculate the values of the RLC lumped circuit elements [20].

$$Q_0 = \frac{f_r}{BW} \tag{3}$$

$$Q_0 = 2\pi f_r RC \tag{4}$$

$$f_r = \frac{1}{2\pi\sqrt{LC}} \tag{5}$$

The resonant frequency, f_r and real part of input impedance R is obtained from Fig. 5 and Fig. 7 respectively at different values of BF_L. The real part of input impedance R is obtained by activating each resonator independently. As seen from Fig. 7, the magnitude of input impedance is approximately equal to 50 Ω at resonance frequencies 6.2, 7.1, 8.2 and 9.5 GHz which is a clear indication of proper impedance matching. By substituting these values in Eq.(3), the quality factor Q_0, for each resonator is obtained. These values are used in (4) and (5) to compute capacitance and inductance.

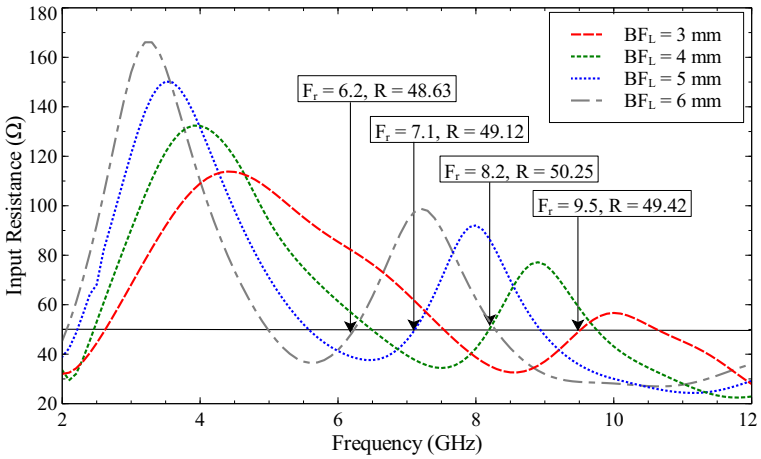

Fig. 7. Antenna input resistance plot.

Table IV lists the antenna equivalent lumped circuit parameters for various values of BF_L. It can be concluded from table IV that different values of BF_L generate different PRLC values which makes BF_L a tuning parameter for the antenna. Fig. 8 shows the ADS simulation results for the reflection

coefficient of the equivalent circuit model which is inline with the simulation results shown in Fig. 5. Thus, from the above discussion, it can be concluded that the equivalent circuit model gives useful information about tuned resonant frequencies and their prominence in relation to input impedance and different values of BF_L.

TABLE IV. ANTENNA EQUIVALENT LUMPED CIRCUIT PARAMETERS

BFL	**Lower Resonance**					**Higher Resonance**				
(mm)	**Fr (GHz)**	**BW (GHz)**	**R (Ω)**	**L (nH)**	**C (pF)**	**Fr (GHz)**	**BW (GHz)**	**R (Ω)**	**L (pH)**	**C (pF)**
3	2.5	1.6	44.47	1.81	2.24	9.5	3	49.42	261.45	1.07
4	2.4	1	45.43	1.26	3.5	8.2	2.1	50.25	255.98	1.51
5	2	0.8	38.92	1.24	5.11	7.1	1.8	49.12	279.15	1.8
6	2	0.6	39.4	0.94	6.73	6.2	1.5	48.63	302.02	2.18

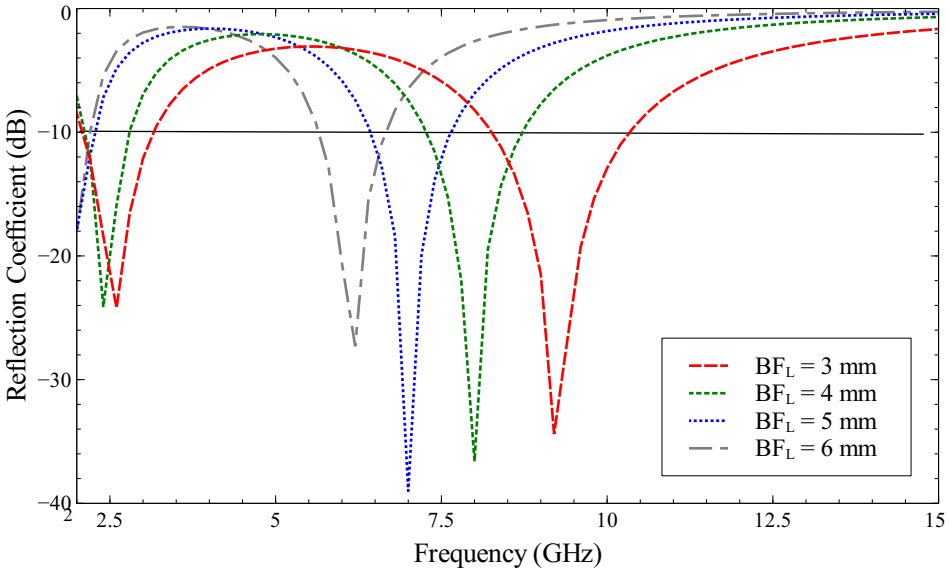

Fig. 8. ADS simulation results for the reflection coefficient.

III. RECONFIGURABLE UWB-NB ANTENNA DESIGN

To evaluate UWB-NB performance using a single antenna, the proposed antenna is simulated with reconfigurable bypass feed length BF_L set to 3 mm, 4 mm, 5 mm and 6 mm using a PIN diode switching network. The implementation results in five modes of operation. Mode-1 provides a sensing antenna in UWB range whereas, Mode-2 to Mode-5 achieves the four different NB ranges. Geometry of the proposed reconfigurable UWB-NB antenna is shown in Fig. 9.

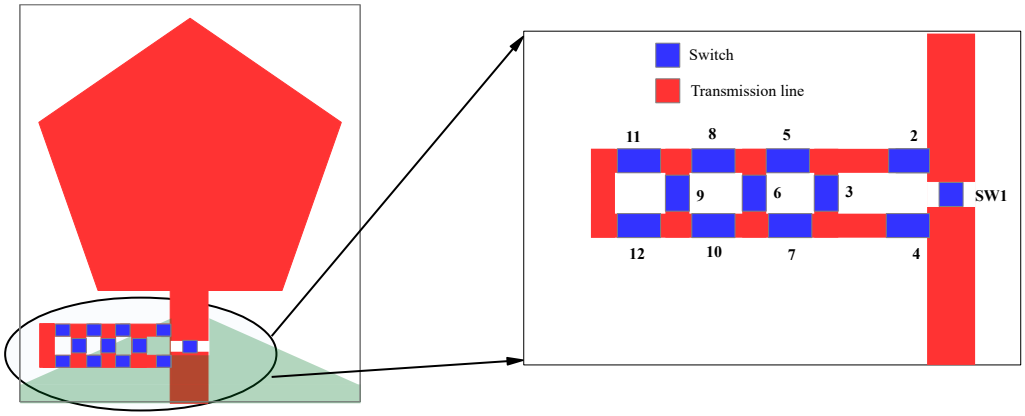

Fig. 9. Geometry of the proposed reconfigurable UWB-NB antenna.

The PIN diode is modeled using a lumped RLC model. The equivalent circuit of the PIN diode when it is in OFF state and ON state is shown in Fig. 10a and Fig. 10b respectively. The PIN diode lumped circuit model used in HFSS is shown in figure 10c. For proof of concept, the various modes have been fabricated wherein ON state of the PIN diode is implemented by shorting the terminals and OFF state implemented by leaving the terminals open. The fabricated antenna in various modes is as shown in Fig. 11. Performance of the simulated and fabricated antenna is evaluated on Ansys HFSS and Keysight VNA E5063A which operate in the frequency range from 100 kHz to 18 GHz. In the simulation, R_S = 1MΩ, L = 0.7 nH and C_T = 0.017 pF for OFF state, whereas, for ON state, R_S = 1 Ω and L = 0.7 nH is used.

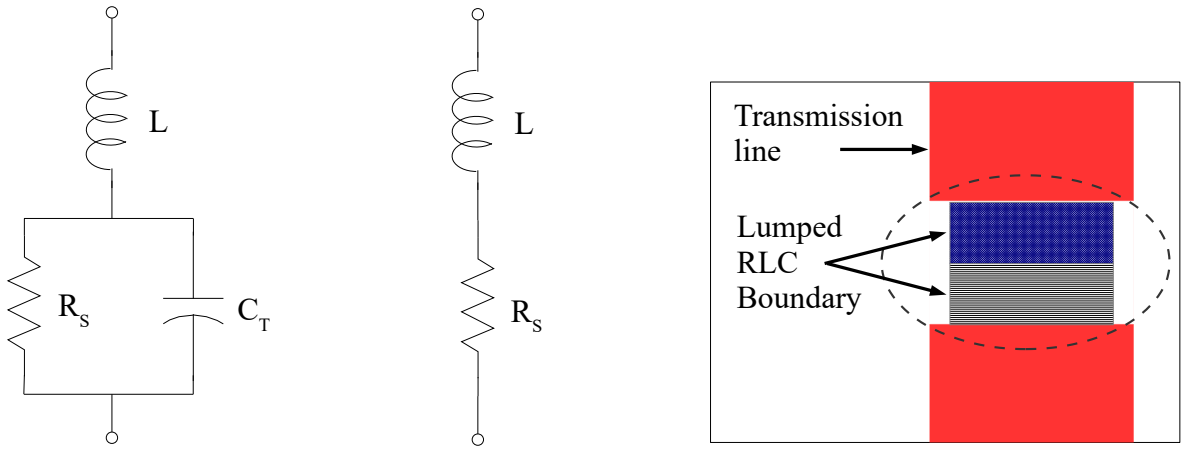

(a) (b) (c)

Fig. 10. Equivalent circuit for PIN diode (a) OFF state, and (b) ON state and, (c) Lumped RLC HFSS model.

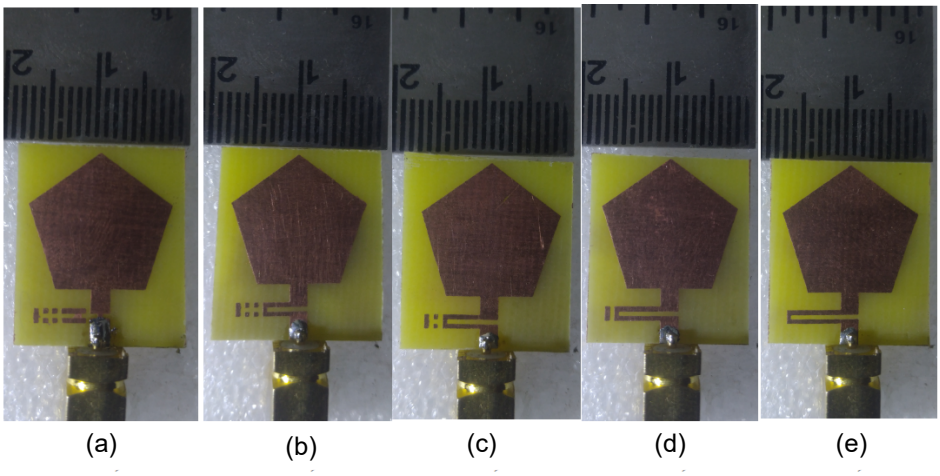

Fig. 11. Fabricated antenna prototype in (a) Mode-1, (b) Mode-2, (c) Mode-3, (d) Mode-4, (e) Mode-5.

Table V shows the state of PIN diodes in various modes and frequency ranges obtained in each mode. Fig. 12 and Fig. 13 shows the simulated and measured reflection coefficient of the UWB-NB antenna respectively. The measurement is carried out over the frequency range from 2 to 18 GHz. When SW1 is in ON state and all the remaining switches are in OFF state, the proposed antenna operates in Mode-1 and the UWB range achieved is from 2.4 to 18 GHz which is 152.4% fractional bandwidth. In Mode-2, SW2 to SW4 are in ON state, and remaining switches are in OFF state. Under this condition, the antenna is connected to a 3 mm bypass feed and SW2 and SW4 are used to bypass the RF signal when SW1 is off. This results in 8.4-11.4 GHz communication range with a 20.2% fractional bandwidth in simulation while 8.6-11.6 GHz with a 19.8% fractional bandwidth obtained in measured results. In Mode-3, the antenna is connected to a 4 mm bypass feed which achieves the frequency range of 7.2 to 8.8 GHz with 20% fractional bandwidth in simulation while 7.6 to 8.8 GHz with a 19.8% fractional bandwidth obtained from the fabricated antenna.

In Mode-4, the antenna is connected to a 5 mm bypass feed and achieves the frequency range of 6.0 to 7.6 GHz with 23.6% fractional bandwidth in simulation while 6.3 to 7.8 GHz with a 23.6% fractional bandwidth obtained from the fabricated antenna. Finally, in Mode-5, bypass feed length is set to 6 mm which helps to achieve the frequency range of 5.3 to 6.8 GHz with 24.8% fractional bandwidth in simulation while 5.8 to 7.1 GHz with a 20.2% fractional bandwidth obtained from the fabricated antenna.

TABLE V. SIMULATION AND MEASURED RESULTS COMPARISON

Mode	ON Switches	OFF Switches	Simulated	Measured
1	SW1	SW2-SW12	2.4-18 GHz	2.4-18 GHz
2	SW2-SW4	SW1, SW5-SW12	8.4-11.4 GHz	8.6-11.6 GHz
3	SW2, SW4, SW5-SW7	SW1, SW3, SW8-SW12	7.2-8.8 GHz	7.6-8.8 GHz
4	SW2, SW4, SW5, SW7, SW8-SW10	SW1, SW3, SW6, SW11, SW12	6.0-7.6 GHz	6.3-7.8 GHz
5	SW2, SW4, SW5, SW7, SW8, SW10, SW11, SW12	SW1, SW3, SW6, SW9	5.3-6.8 GHz	5.8-7.1 GHz

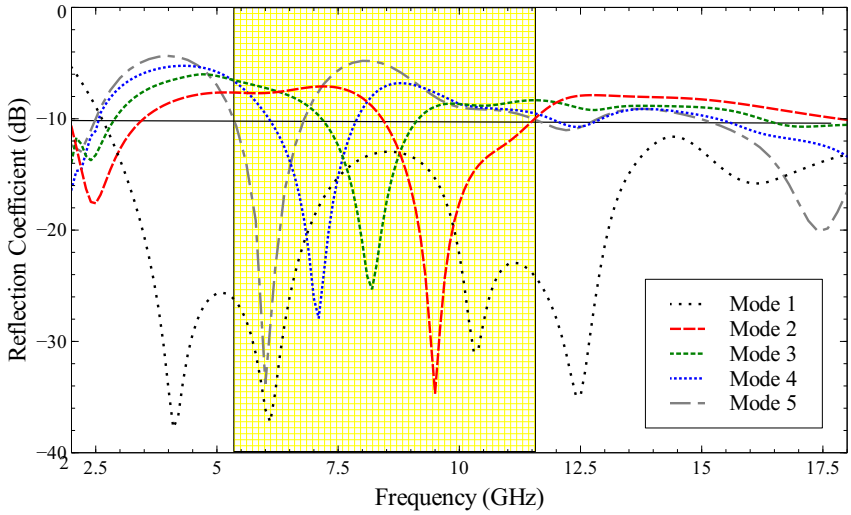

Fig. 12. Simulated reflection coefficient for different operating modes.

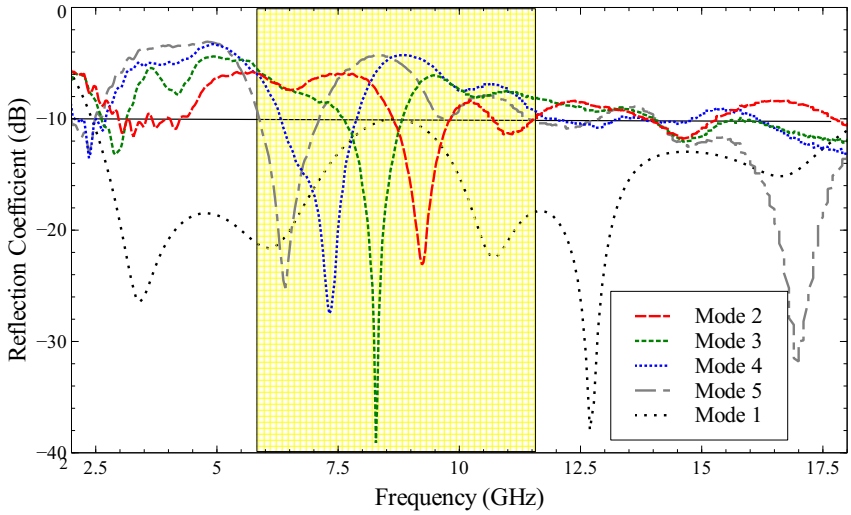

Fig. 13. Measured reflection coefficient for different operating modes.

Fig. 14 and Fig. 15 shows the normalized simulated and measured far-field radiation patterns of the proposed antenna respectively in the different operating modes. The radiation pattern of the proposed antenna is simulated and measured in UWB Mode-1 at 3 GHz, 4.5 GHz, 8 GHz, 15 GHz in XZ-plane (H-plane) and YZ-plane (E-plane) respectively. The radiation pattern of the proposed antenna is simulated and measured in Mode-2 to Mode-5 at 6.2 GHz, 7.1 GHz, 8.2 GHz and 9.5 GHz in XZ-plane (H-plane) and YZ-plane (E-plane) respectively. Radiation pattern in the E-plane is bi-directional and the pattern is omnidirectional in the H-plane over the entire operating modes. The omnidirectional radiation pattern confirms that the proposed antenna is highly suitable for handheld applications.

ISSN 2179-1074

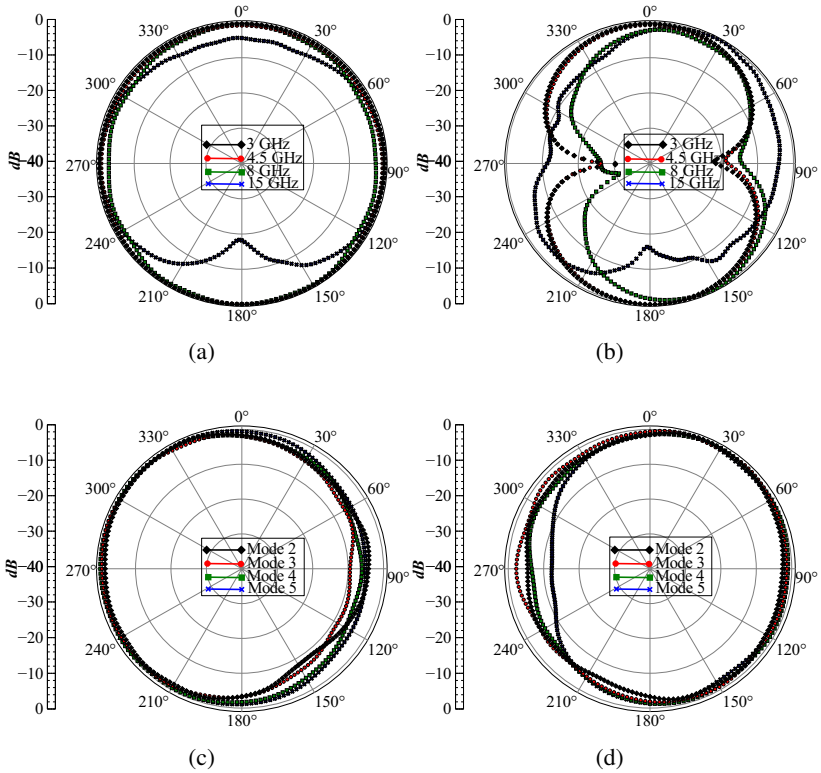

Fig. 14. Simulated normalized radiation pattern of the proposed antenna (a) Mode-1 in H-plane, (b) Mode-1 in E-plane, (c) Mode-2 to Mode-5 in H-plane and (d) Mode-2 to Mode-5 in E-plane.

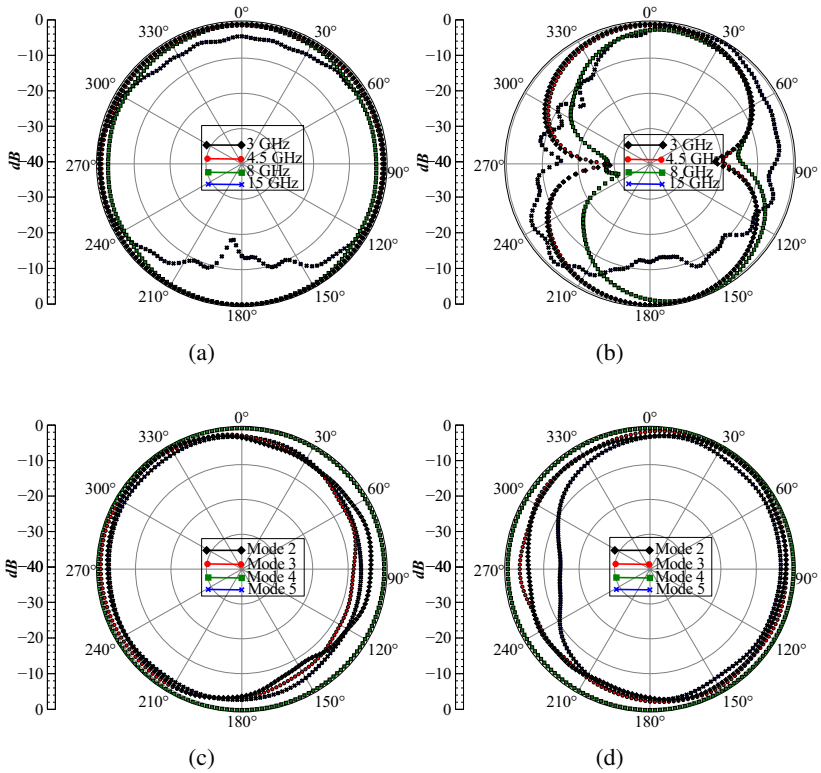

Fig. 15. Measured normalized radiation pattern of the proposed antenna (a) Mode-1 in H-plane, (b) Mode-1 in E-plane, (c) Mode-2 to Mode-5 in H-plane and (d) Mode-2 to Mode-5 in E-plane.

IV. CONCLUSION

In this paper, single port, low profile, low cost, multimode, reconfigurable UWB-NB antenna suitable for applications such as handheld Cognitive Radio is presented. The antenna is composed of a pentagonal patch excited by the microstrip feedline integrated with a reconfigurable bypass feed network. The frequency reconfiguration is achieved by selecting the relevant RF path using a network of PIN diodes. The antenna provides a single UWB frequency (2.4 to 18 GHz) and four NB frequencies (5.3 to 6.8, 6.0 to 7.6, 7.2 to 8.8 and 8.4 to 11.4 GHz) with omnidirectional radiation pattern. The fabricated antenna is low profile with dimensions $18\times21\times1.6$ mm^3. The performance of the fabricated antenna is inline with the simulated antenna. The antenna achieves a gain from 2.2 to 6.2 dBi with a maximum gain at 12 GHz. The overall radiation efficiency of the antenna is found to be in the range of 70 to 90%.

REFERENCES

[1] S. Haykin, "Cognitive radio: brain-empowered wireless communications," *IEEE journal on selected areas in communications*, vol. 23, no. 2, pp. 201–220, 2005.

[2] H. A. Atallah, A. B. Abdel-Rahman, K. Yoshitomi, and R. K. Pokharel, "Compact frequency reconfigurable filtennas using varactor loaded T-shaped and H-shaped resonators for cognitive radio applications," *IET Microwaves, Antennas & Propagation*, vol. 10, no. 9, pp. 991–1001, 2016.

[3] P.-Y. Qin, F. Wei, and Y. J. Guo, "A wideband-to-narrowband tunable antenna using a reconfigurable filter," *IEEE Transactions on Antennas and Propagation*, vol. 63, no. 5, pp. 2282–2285, 2015.

[4] I. Shah, S. Hayat, A. Basir, M. Zada, S. Shah, and S. Ullah, "Design and analysis of a hexa-band frequency reconfigurable antenna for wireless communication," *AEU-International Journal of Electronics and Communications*, vol. 98, pp. 80–88, 2019.

[5] N. AL-Fadhali, H. A. Majid, R. Omar, S. H. Dahlan, A. Y. Ashyap, S. M. Shah, M. K. Rahim, and B. A. Esmail, "Substrate integrated waveguide cavity backed frequency reconfigurable antenna for cognitive radio applies to internet of things applications," *International Journal of RF and Microwave Computer-Aided Engineering*, vol. 30, no. 1, p. e22020, 2020.

[6] S. Kingsly, D. Thangarasu, M. Kanagasabai, M. G. N. Alsath, R. R. Thipparaju, S. K. Palaniswamy, and P. Sambandam, "Multiband reconfigurable filtering monopole antenna for cognitive radio applications," *IEEE Antennas and Wireless Propagation Letters*, vol. 17, no. 8, pp. 1416–1420, 2018.

[7] Z. Mahlaoui, E. Antonino-Daviu, M. Ferrando-Bataller, H. Benchakroun, and A. Latif, "Frequency reconfigurable patch antenna with defected ground structure using varactor diodes," in *2017 11th European Conference on Antennas and Propagation (EUCAP)*, pp. 2217–2220, 2017.

[8] C. Guo, L. Deng, J. Dong, T. Yi, C. Liao, S. Huang, and H. Luo, "Variode enabled frequency-reconfigurable microstrip patch antenna with operation band covering S and C bands," *Progress In Electromagnetics Research*, vol. 88, pp. 159–167, 2020.

[9] E. Ebrahimi, J. R. Kelly, and P. S. Hall, "Integrated wide-narrowband antenna for multi-standard radio," *IEEE transactions on antennas and propagation*, vol. 59, no. 7, pp. 2628–2635, 2011.

[10] R. Hussain and M. S. Sharawi, "A cognitive radio reconfigurable MIMO and sensing antenna system," *IEEE Antennas and Wireless Propagation Letters*, vol. 14, pp. 257–260, 2014.

[11] A. Gandhi and N. Anveshkumar, "A planar four-port integrated UWB and NB antenna system for CR in 3.1 GHz to 10.6 GHz," in *2019 National Conference on Communications (NCC)*, pp. 1–6, 2019.

[12] A. Nella and A. S. Gandhi, "A five-port integrated UWB and narrowband antennas system design for CR applications," *IEEE Transactions on Antennas and Propagation*, vol. 66, no. 4, pp. 1669–1676, 2018.

[13] M. Abioghli, A. Keshtkar, M. Naser-Moghadasi, and B. Ghalamkari, "UWB rectangular DRA integrated with reconfigurable narrowband antenna for cognitive radio applications," *IETE Journal of Research*, pp. 1–9, 2018.

[14] M. Bitchikh, W. Rili, and M. Mokhtar, "An UWB to narrow band and Bi-bands reconfigurable octogonal antenna," *Progress In Electromagnetics Research*, vol. 74, pp. 69–75, 2018.

[15] A. Mansoul, F. Ghanem, M. R. Hamid, and M. Trabelsi, "A selective frequency-reconfigurable antenna for cognitive radio applications," *IEEE antennas and wireless propagation letters*, vol. 13, pp. 515–518, 2014.

Brazilian Microwave and Optoelectronics Society-SBMO *received 21 May 2022; for review 5 June 2022; accepted 24 Oct 2022*
Brazilian Society of Electromagnetism-SBMag *ISSN 2179-1074*

[16] B.-J. Liu, J.-H. Qiu, S.-C. Lan, and G.-Q. Li, "A wideband-to-narrowband rectangular dielectric resonator antenna integrated with tunable bandpass filter," *IEEE Access*, vol. 7, pp. 61 251–61 258, 2019.

[17] P. Kabacik and M. E. Bialkowski, "The temperture dependence of substrate parameters and their effect on microstrip antenna performance," *IEEE Transactions on Antennas and Propagation*, vol. 47, no. 6, pp. 1042–1049, 1999.

[18] M. Sherman, A. N. Mody, R. Martinez, C. Rodriguez, and R. Reddy, "IEEE standards supporting cognitive radio and networks, dynamic spectrum access, and coexistence," *IEEE Communications Magazine*, vol. 46, no. 7, pp. 72–79, 2008.

[19] K. P. Ray, "Design aspects of printed monopole antennas for ultra-wide band applications," *International journal of antennas and propagation*, vol. 2008, 2008.

[20] M. Rahman, W. T. Khan, and M. Imran, "Penta-notched UWB antenna with sharp frequency edge selectivity using combination of SRR, CSRR, and DGS," *AEU-International Journal of Electronics and Communications*, vol. 93, pp. 116–122, 2018.

  ISSN 2179-1074